ICMNS Bcrec

by Steky Steky

Submission date: 27-Nov-2018 10:57PM (UTC+0700)
Submission ID: 1045700907
File name: Paper_Steky_BCREC.docx (1.39M)
Word count: 2436
Character count: 14271

bcl Morphology Formation Strategy on Nanostructured Titania via Alkaline Hydrothermal Treatment

Fry V. Steky[1], Veinardi Suendo[1,2 *], Rino R. Mukti[1,2], Didi P. Benu[1], Muhammad Reza[1], Damar R. Adhika[2], Viny V. Tanuwijaya[2], Ashari B. Nugraha[2]

[1] *Division of Inorganic and Physical Chemistry, Faculty of Mathematics and Natural Sciences, Institut Teknologi Bandung, Jl. Ganesha No. 10, Bandung 40132 Indonesia*

[2] *Research Center for Nanosciences and Nanotechnology, Institut Teknologi Bandung, Jl. Ganesha No 10, Bandung 40132, Indonesia*

* *Corresponding Author. E-mail: vsuendo@chem.itb.ac.id / Veinardi.Suendo@polytechnique.edu (V. Suendo),*

Phone: +62-22-2502103, Fax: +62-22-2504154

Abstract

Titanium dioxide (TiO_2) is a semiconductor material that plays an important role in photocatalysis. Bicontinuous concentric lamellar (*bcl*) is an interesting morphology with open channel pore structure that has been successfully synthesized on silica-based materials. If *bcl* morphology can be applied in TiO_2 system, then many surface properties of TiO_2 can be enhance, i.e. photocatalytic activity. A simple and effective strategy has been demonstrated to transform aggregated and spherical TiO_2 particles to *bcl* morphology via alkaline hydrothermal route. Alkaline hydrothermal treatment successfully transforms TiO_2 particle surface to have *bcl* morphology through swelling with ammonia then followed by phase segregation process. We proposed this strategy as a general pathway to transform the particle surface with any shape to have *bcl* morphology.

Keywords:

Alkaline hydrothermal treatment; *bcl* morphology; lamellar morphology; modified morphology, nanostructured TiO_2

1. Introduction

Titanium dioxide (TiO_2) is an important inorganic semiconductor material in various applications due to its photosensitive, photostable, and environmentally friendly properties [1]. The advantages properties of TiO_2 provide potential applications in many fields such as photocatalysts [2], dye-

sensitized solar cells [3], and catalyst support [4]. Due to its wide application, research about synthesis, characterization and fundamental understanding of TiO_2 material has been intensively studied in last recent years. Many researchers developed TiO_2 synthesis methods to enhance the TiO_2 activity in various applications [5] [6], especially as photocatalysts.

Many research groups reported that particle size and morphology are important to obtain TiO_2 with good photocatalytic activity [7-9]. The effective charge transfer in photocatalyst TiO_2 requires the presence of surface active sites [10]. The essential requirement to have a high surface active sites photocatalyst is to have a high surface area. The common strategy to increase surface area is by reducing the crystallite size. However, small TiO_2 particles have low mechanical strength and easily agglomerate to form larger particles. We can use another strategy to increase the surface area of TiO_2 particles by modifying its morphology. Conventional mesoporous TiO_2 has only closed channel pore structure from intercrystallite spaces. However, closed channel pore structure has several drawbacks, such low accessibility due to diffusion limitation, pore blocking, and difficult pore surface activation, despite its high selectivity. Therefore, in vast reaction schemes, open channel is more favorable. TiO_2 particles with open channel structure provide high surface area, high accessibility and facile pore surface modification [11]. Photocatalytic activity of mesoporous materials with open channel pore structure is easy to adjust chemically due to large reachable surfaces [12].

One of morphology with open channel pore structure that attracts much attention is bicontinuous concentric lamellar (*bcl*) morphology. *bcl* morphology has been successfully synthesized in various type silica-based materials using reverse micelle templating method [13]. The morphology of *bcl* silica is quite unique. Here, uniform spherical particles consist of bicontinuous lamellae arranged concentrically providing high surface area, large pore volume, and high accessibility [13]. If this morphology can be applied in TiO_2 system, then many surface properties of TiO_2 can be enhance, i.e. photocatalytic activity. Synthesis of TiO_2 with reverse micelle has been reported elsewhere, but only TiO_2 particles with irregular morphology obtain in the form of aggregates. This type of particles provide low photocatalytic activity [14]. *bcl* morphology cannot be obtain using the reverse micelle templating due to the hydrolysis nature of TiO_2 precursors, i.e. $TiCl_4$, TTIP, etc. It is a rule of thumb that TiO_2 precursors hydrolysis rapidly event in the traces of water.

Herein, synthesis of nanostructured TiO_2 with *bcl* morphology will be carried out in two simple steps without surfactant. Slow hydrolysis will be the main strategy to form TiO_2 particles with controllable particle shape. Swelling and phase segregation will be the key to obtain bicontinuous lamellar morphology.

2. Materials and Methods

2.1. Preparation of Nanostructured TiO_2 with *bcl* Morphology

Titanium dioxide was synthesized by modifying previously reported method [5]. First, 1.1 mL of Titanium (IV) Isopropoxide (TTIP, 99%, Sigma–Aldrich) was added to 100 mL of ethanol (99%, Merck) under vigorous stirring for 30 minutes. Formed milky white suspension was kept static for 24 hours and then filtered. The powder obtained was washed with deionized (DI) water and ethanol, and dried at 60 °C overnight. Then, 0.3 g of as-prepared TiO_2 was dissolved in 24 mL of ammonia (25%, Sigma–Aldrich) together with 12 mL of DI water. The mixture was then transferred to a 50 mL Teflon-line stainless steel autoclave, heated to 120 °C and kept static for 6 hours. After this treatment, the autoclave was cooled down to room temperature naturally. The obtained products were filtered and washed with DI water and ethanol. Finally, the prepared powders were calcined at 500 °C for 1 hours. All the steps above are repeated using the same method with absolute ethanol is replaced by DI water.

Within this study, the samples are designated as TiO_2-A (aggregate), TiO_2-S (sphere), TiO_2-A-HT (aggregate after hydrothermal treatment), TiO_2-S-HT (sphere after hydrothermal treatment), TiO_2-A-HT-500 (aggregate after hydrothermal and calcination), and TiO_2-S-HT-500 (sphere after hydrothermal and calcination).

2.2. Sample Characterizations

The morphology of obtained samples were characterized with scanning electron microscopy (SEM, Hitachi SU3500) with the accelerating voltage at 10 kV. The phase structures were determined by Raman spectroscopy (Bruker – Senterra) with a 532 nm Nd:YAG DPSS (diode-pumped solid-state) laser at 2 mW on 5s scanning time and X-ray diffraction (XRD, Bruker D8 Advance with LynxEye XE detector) on a Scintag diffractometer with CuKα1 radiation (λ = 1.54060 Å) at a scanning rate of 0.239° s^{-1} in the 2θ range from 10 to 90°.

3. Results and Discussion

Nanostructured TiO_2 with *bcl* morphology was prepared as explained in the Experimental Section. As shown in Figure 1a and 1b, the aggregate and spherical shape particles were investigated by SEM. The main difference in preparation condition between two kinds of resulted particles is the hydrolysis rate of TiO_2 precursor. TTIP dissolved in DI water experiences rapid hydrolysis, thus produces aggregated particles with irregular shape. On the other hand, if DI water was replaced by ethanol, TTIP experiences a slow hydrolysis pathway producing spherical particles.

Figure 1c and 1d show the morphology of particles after alkaline hydrothermal treatment. We observed the surface of both aggregates and spherical particles transform into bicontinuous lamellar morphology. Alkaline hydrothermal treatment has been proved to be independent of particle shape and synthesis history. As long as the particles have not been calcined yet, then the method can be applied.

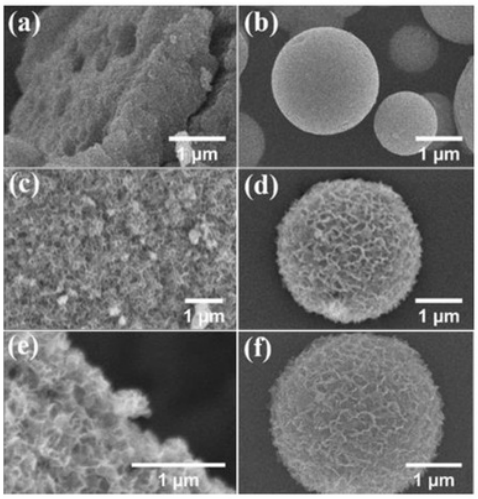

Figure 1. SEM images of nanostructured TiO_2 obtained after different processes: (a) TiO_2-A, (b) TiO_2-S, (c) TiO_2-A-HT, (d) TiO_2-S-HT, (e) TiO_2-A-HT-500 and (f) TiO_2-S-HT-500.

Based on results above, we hypothesized that the formation of these lamellar structures were carried out by chemically modifying the surface of particles through swelling and phase segregation under alkaline condition. Figure 1e and 1f shows the SEM images of samples after calcination at 500 °C for 6 h. Both images show no significant changes in their morphology after calcination process with respect to Figure 1c and 1d, respectively. Although SEM images do not show noticeable morphology changes after calcination process, Raman and XRD analysis reveal significant differences (Figure 2 and 3).

Figure 2a shows Raman spectra of synthesized TiO_2 samples. In principle, Raman analysis is not a sensitive method to distinguish particle morphology, i.e. both uncalcined aggregated and spherical particles give relatively similar Raman spectra. However, Raman is very sensitive to distinguish different chemical components and polymorphism in crystalline materials, i.e. between anatase and rutile TiO_2 polymorphs.

Although all uncalcined samples look very similar, after alkaline hydrothermal treatment samples show several different features in their Raman spectra. These features might due to the formation of ammonium titanate during alkaline hydrothermal treatment.14 Moreover, aggregated particles (TiO_2-A-HT) provide spectra with richer features and sharper peaks with respect to spherical particles

(TiO_2-S-HT). This might due the aggregated particles have more defects on their surfaces, which is in good agreement with SEM results depicted in Figure 1c and 1d, respectively.

After calcined samples demonstrate typical anatase peaks with Raman shift at 154.50 cm-1; 206.04 cm-1, 396.18 cm-1, 513.34 cm-1 and 631. 73 cm-1 that assigned to the vibrational modes Eg(1), Eg(2), B1g(1), B1g(2)+A1g, and Eg(3), respectively. These peaks represents the vibrational normal modes of anatase as depicted schematically in Figure 2b. Rutile peaks cannot be observed in calcined sample without deconvolution. In other hand, there is no anatase or rutile peaks can be observed in Raman spectra of uncalcined samples.

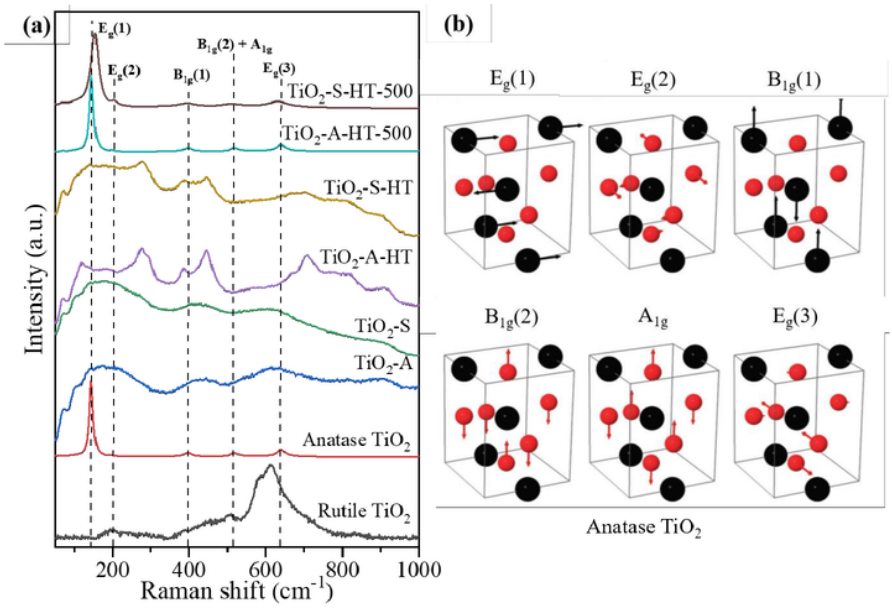

Figure 2. (a) Raman spectra of standard anatase and rutile TiO_2, TiO_2-A, TiO_2-S, TiO_2-A-HT, TiO_2-S-HT, TiO_2-A-HT-500, TiO_2-S-HT-500 and (b) schematic of anatase vibrational modes [15].

To get more structural insights of synthesized TiO_2, XRD analysis has to be performed. Figure 3 shows the diffractogram of all samples, including the reference standard of rutile and anatase polymorphs. The inset of Figure3 shows the crystal structure of anatase and rutile. Uncalcined samples demonstrate similar XRD pattern consists of three broad amorphous peaks. The calcined samples show dominant anatase phase with a trace rutile phase. The peaks at 25.30°, 36.90°, 37.77°, 38.68°, 48.05°, 53.87°, 55.08°, 62.10°, 62.68°, 68.74°, 70.31°, 75.04°, 76.08°, and 82.70° are assigned to the anatase phase. A trace peak at 27.48° is assigned to the rutile phase.

Based on XRD and Raman analysis results, we propose that the structural precursor of anatase phase obtained after calcination were already resided in all uncalcined samples. The structural precursor feature is more pronounced in XRD than in Raman results, represents by three broad

amorphous peaks. Structural precursor appears in Raman spectra only as a broad background. Alkaline hydrothermal treatment does not alter much this feature in XRD pattern, only one additional peak appears around 48.05°, represents the anatase phase. This structural precursor feature can be used to indicate where the calcination process will terminate. In this case, the calcination of this material will lead mainly to the formation of anatase phase.

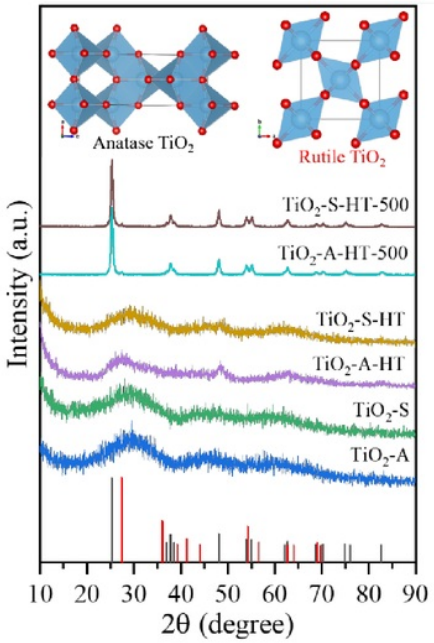

Figure 3. XRD pattern of standard anatase and rutile TiO_2, TiO_2-A, TiO_2-S, TiO_2-A-HT, TiO_2-S-HT, TiO_2-A-HT-500, and TiO_2-S-HT-500 with anatase and rutile structures.

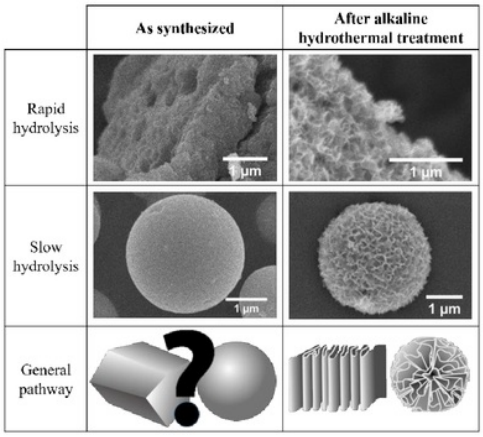

Figure 4. Schematic of TiO_2 synthesis route to produce different particle shape with *bcl* morphology.

Although the particles growth mechanism is still obscure, we proposed a general pathway based on *bcl* silica mechanism13 and this results, to transform any particle shape to *bcl* morphology (Figure 4). Here, we succeeded to demonstrate the transformation of aggregated and spherical particles to *bcl* morphology via alkaline hydrothermal route.

4. Conclusions

A simple and effective strategy has been demonstrated to transform aggregated and spherical particles to *bcl* morphology via alkaline hydrothermal route. We proposed this strategy as a general pathway to transform the particle surface with any shape to have *bcl* morphology. This proposed synthesis strategy will open a new perspective in the development of mesoporous materials with open channel pore structure and their applications in vast variety of fields.

Acknowledgments

This research was financially supported by ITB Research Grant 2018 as a part of ITB Research and Inovation Program 2018. F. V. Steky acknowledges Directorate General of Higher Education for Bidikmisi scholarship. Muhammad Reza acknowledges Ministry of Education and Culture of Indonesia for scholarship through Beasiswa Unggulan. D. P. Benu acknowledges Lembaga Pengelola Dana Pendidikan (LPDP) for scholarship support. Authors also acknowledge financial support from Faculty of Mathematics and Natural Sciences, Institut Teknologi Bandung for participation in ICMNS 2018.

References

[1] Yeh, S. W., Ko, H. H., Chiang, H. M., Chen, Y. L., Lee, J. H., Wen, C. M., Wang, M. C. (2014). Characteristics and Properties of a Novel In Situ Method of Synthesizing Mesoporous TiO_2 Nanopowders by a Simple Coprecipitation Process without Adding Surfactant. *Journal of Alloys and Compounds*, 613: 107–116.

[2] Liu, G., Liu, L., Song, J., Liang, J., Luo, Q., & Wang, D. (2014). Visible Light Photocatalytic Activity of TiO_2 Nanoparticles Hybridized by Conjugated Derivative of Polybutadiene. *Superlattices and Microstructures*, 69: 164–174.

[3] Latini, A., Cavallo, C., Aldibaja, F.K., Gozzi, D. (2013). Efficiency Improvement of DSSC Photoanode by Scandium Doping of Mesoporous Titania Beads. *J. Phys. Chem. C*, 117: 25276−25289.

[4] Hao, C., Lv, H., Mi, C., Song, Y., Ma, J. (2016). Investigation of Mesoporous Niobium-Doped TiO_2 as an Oxygen Evolution Catalyst Support in an SPE Water Electrolyzer. *ACS Sustainable*

Chem. Eng.: 4, 746–756.

[5] Jitputti, J., Rattanavoravipa, T., Chuangchote, S., Pavasupree, S., Suzuki, Y., Yoshikawa, S., Qiu, J. (2009). Fabrication of Size-Controllable Flower-Like TiO_2 and Its Photocatalytic Activity. *Journal of the American Ceramic Society*, 16: 3–9.

[6] Chen, X., Mao, S. S. (2007). Titanium Dioxide Nanomaterials: Synthesis, Properties, Modifications, and Applications. *Chem. Rev.*, 107: 2891-2959.

[7] Lee, J., Orilall, M.C., Warren, S.C., Kamperman, M., DiSalvo, F.J., Wiesner, U. (2008). Direct access to thermally stable and highly crystalline mesoporous transition-metal oxides with uniform pores. *Nat. Mater*, 7: 222-228.

[8] Zhou, H. S., Li, D. L., Hibino, M., Honma, I. (2005). A self-ordered, crystalline-glass, mesoporous nanocomposite for use as a lithium-based storage device with both high power and high energy densities. *Angew. Chem., Int. Ed*, 44: 797-802.

[9] Alivov, Y., Fan, Z. Y. (2009). A Method for Fabrication of Pyramid-Shaped TiO_2 Nanoparticles with a High {001} Facet Percentage. *J. Phys. Chem. C*., 113: 12954–12957.

[10] Nowotny, J., Bak, T., Nowotny, M. K., Sheppard, L. R. (2006). TiO_2 Surface Active Sites for Water Splitting. *J. Phys. Chem. B*, 110: 18492-18495

[11] Bayal, N., Singh, R., Polshettiwar, V. (2017). Nanostructured Silica-Titania Hybrid using Fibrous Nanosilica as Photocatalysts. *ChemSusChem*, 10: 2182-2191.

[12] Dhiman, M., Chalke, B., Polshettiwar, V. (2015). Efficient Synthesis of Monodisperse Metal (Rh, Ru, Pd) Nanoparticles Supported on Fibrous Nanosilica (KCC-1) for Catalysis. *ACS Sustainable Chem. Eng.*, 3: 3224−3230

[13] Febriyanti, E., Suendo, V., Mukti, R. R., Prasetyo, A., Arifin, A. F., Akbar, M. A., Marsih, I. N. (2016). Further Insight on the Definite Morphology and Formation Mechanism of Mesoporous Silica KCC-1. *Langmuir*, 32: 5802-5811.

[14] Inaba, R., Fukahori, T., Hamamoto, M., & Ohno, T. (2006). Synthesis of Nanosized TiO_2 Particles in Reverse Micelle Systems and Their Photocatalytic Activity for Degradation of Toluene in Gas Phase. *Journal of Molecular Catalysis A: Chemical*, 260: 247–254.

[15] Frank, O., Zukalova, M., Laskova, B., Kurti, J., Koltai, J., Kavan, L. (2012). Raman Spectra of Titanium Dioxide (Anatase, Rutile) with Identified Oxygen Isotopes (16, 17, 18). *Phys. Chem. Chem. Phys.*, 14: 14567–14572.

ICMNS Bcrec

ORIGINALITY REPORT

19%	8%	18%	3%
SIMILARITY INDEX	INTERNET SOURCES	PUBLICATIONS	STUDENT PAPERS

PRIMARY SOURCES

1	Zhang, Wei, Weidong Zhou, Jaspher H Wright, Yongnam Kim, Dawei Liu, and Xingcheng Xiao. "Mn-doped TiO2 Nanosheet-based Spheres as Anode Materials for Lithium-ion Batteries with High Performance at Elevated Temperatures", ACS Applied Materials & Interfaces Publication	8%
2	Febriyanti, Erna, Veinardi Suendo, Rino R. Mukti, Anton Prasetyo, Adry Fahmi Arifin, Muhamad Ali Akbar, Sugeng Triwahyono, I Nyoman Marsih, and - Ismunandar. "Further Insight on the Definite Morphology and Formation Mechanism of Mesoporous Silica KCC-1", Langmuir, 2016. Publication	2%
3	Wei Zhang, Dawei Liu. "Nitrogen-treated Hierarchical Macro-/Mesoporous TiO2 Used as Anode Materials for Lithium Ion Batteries with High Performance at Elevated Temperatures", Electrochimica Acta, 2015 Publication	1%

4	Juan Felipe Montoya, Irina Ivanova, Ralf Dillert, Detlef W. Bahnemann, Pedro Salvador, José Peral. " Catalytic Role of Surface Oxygens in TiO Photooxidation Reactions: Aqueous Benzene Photooxidation with Ti O under Anaerobic Conditions ", The Journal of Physical Chemistry Letters, 2013 Publication	1%
5	Fattakhova-Rohlfing, Dina, Adriana Zaleska, and Thomas Bein. "Three-Dimensional Titanium Dioxide Nanomaterials", Chemical Reviews Publication	1%
6	dyuthi.cusat.ac.in Internet Source	1%
7	Wei Zhang, Yuxuan Gong, Nathan P. Mellott, Dawei Liu, Jiangang Li. "Synthesis of nickel doped anatase titanate as high performance anode materials for lithium ion batteries", Journal of Power Sources, 2015 Publication	1%
8	Journal of Information, Communication and Ethics in Society, Volume 12, Issue 3 (2014-09-16) Publication	1%
9	www.mrs.org.sg Internet Source	1%

10	A R Luz, C M Lepienski, S L Henke, C R Grandini, N K Kuromoto. "Effect of microstructure on the nanotube growth by anodic oxidation on Ti-10Nb alloy", Materials Research Express, 2017 Publication	<1%
11	G. Murugadoss, R. Jayavel, M. Rajesh Kumar. "Systematic investigation of structural and morphological studies on doped TiO2 nanoparticles for solar cell applications", Superlattices and Microstructures, 2014 Publication	<1%
12	docslide.us Internet Source	<1%
13	epdf.tips Internet Source	<1%
14	oatext.com Internet Source	<1%
15	research-repository.st-andrews.ac.uk Internet Source	<1%
16	pubs.acs.org Internet Source	<1%
17	Nanotechnology for Sustainable Development, 2014. Publication	<1%

Exclude quotes	On	Exclude matches	Off
Exclude bibliography	On		